

CORROSION 2007

PAPER NO. 07450

WATERSIDE BOILER TUBE FAILURE SYMPOSIUM (TEG 163X; STG 11)

FAILURE ANALYSIS AND INVESTIGATION METHODS FOR BOILER TUBE FAILURES

Mehrooz Zamanzadeh, Edward S. Larkin, and George T. Bayer
Matco Associates, Inc.
4640 Campbells Run Road
Pittsburgh, Pennsylvania 15205

William J. Linhart
Allegheny Energy
800 Cabin Hill Drive
Greensburg, Pennsylvania 15601

FAILURE ANALYSIS AND INVESTIGATION METHODS FOR BOILER TUBE FAILURES

Mehrooz Zamanzadeh, Edward S. Larkin, and George T. Bayer
Matco Associates, Inc.
4640 Campbells Run Road
Pittsburgh, Pennsylvania 15205

William J. Linhart
Allegheny Energy
800 Cabin Hill Drive
Greensburg, Pennsylvania 15601

ABSTRACT

Failure analysis methodology is applied to the principal mechanisms by which boiler tubes fail during service. Several important factors often associated with component failures are deficiency in design, fabrication, operating conditions, unsuitable materials selection, and expended useful life. These factors are of primary consideration. The failure analysis procedure, or methodology for evaluation, is provided in a step by step approach. This includes justification for conducting a failure analysis investigation, developing a logical plan for the investigation to follow, collection of background information, sample removal techniques, on-site inspection, laboratory testing and analysis, and the formulation of final report based on relevant data, analysis, and recommendations. Among the case histories discussed are: fatigue, erosion, short-term overheating, and hydrogen damage.

Keywords: failure analysis, boiler tubes, fatigue, erosion, short-term overheating, hydrogen damage.

INTRODUCTION

Failure analysis, and the principal mechanisms by which boiler tubes fail in service, will be examined in this introductory survey. As this is an introductory survey, the reader is referred to two excellent reference texts covering the field of boiler failures for more detailed information. These are the texts authored by French¹ and by Port and Herro². Deficiencies in design, fabrication, operating conditions, unsuitable materials selection, and expended useful life are important factors to consider not only for boiler tubes, but operational components in general. Thus, the failure analyst must consider them of primary importance when a failure occurs in a boiler. If identified early, potential failures or accidents can often be prevented, and as a result costly repair expenses, lost revenue, and legal expenses may be avoided.

To investigate a failure, and analyze the conditions that promoted the failure, important information must be collected on the failed component. Background information on the make and model of the boiler and the tube, specifications, the service history, and physical evidence of the failed part are necessary components to determine

why, how, when, and where a failure may have occurred. If these answers are provided during the course of the investigation, future failures may be better understood or possibly prevented.

The conditions that promoted the failure are essential in identifying the underlying factors that may have initiated the failure. Other elements that may not be readily acknowledged in failure analysis, yet are no less important, are common sense, a critical and unbiased mode of thinking, experience, knowledge, and experimental observation.

Provided in this survey is a step by step approach to failure analysis investigation. The accepted theories and mechanisms, which cause boiler components to fail, will be explored in this paper.

FAILURE ANALYSIS

A failure analysis investigation is much like the work of a detective. Clues or relevant facts pertaining to the investigation must be gathered, analyzed, explored, and studied to make a knowledgeable determination. As in the case of a good detective, first hand field experience is of the utmost importance, yet academic studies are also essential.

A background and thorough understanding of materials used in construction, physical and mechanical properties of materials and their production, fabrication and performance characteristics of the materials, as well as a working knowledge concerning machinery and structural design, and the application and distribution of stresses resulting from service loads as they relate to the properties of materials are vital to fully develop as a successful failure investigator.

In conjunction, a failure analyst must have a procedure; or more precisely, a method for evaluation when a failure occurs. If a product does not live up to its full life expectancy, there must be an evaluation procedure that will identify the loss. A method of evaluation that is logical and well planned will enable the analyst to determine the underlying contributing factors, and provide valid information about the failure for future reference.

Failure Determination

Determining that a failure indeed occurred is the first step in the method for evaluation. In the case of a boiler tube, a failure has occurred if the tube develops a leak, breaks into two or more pieces, if it has physical signs of deterioration that will result in an unsafe environment, or it is incapable of performing its intended function.

If the boiler tube breaks into two or more pieces, it is called a fracture failure. A fracture failure occurs by means of the formation and propagation of cracks resulting in the separation of two or more parts. Several factors that may produce this type of failure are mechanical stresses, environmental or chemical influences, or the effect of heat on the boiler tube. For a failure to be identified as a fracture failure, the item does not have to be completely broken. One small imperfection can jeopardize the entire system.

Once it has been determined that a failure has indeed occurred, the point of origin must be found, and a determination must be made as to whether the failure occurred as a result of design, method of manufacturing, service history and conditions, water chemistry excursions, or from a deficiency in the material. When the point of origin is located, the investigation may proceed to a study of how the failure occurred, possible causes or factors in the failure, and possible means of preventative measures.

Why a failure occurs is an important question in the method of evaluation. This question can be approached by breaking down the failure into "mode of failure" and "cause of failure." Mode of failure is the process by which the failure occurred. Cause of failure is that which can be fixed or changed to prevent future failures. Each question provides important clues to the investigation, and although priorities may be quite different, each question must be addressed and resolved to determine why a failure may have occurred.

In a fracture failure clues to the mode of failure can be revealed by fractography, while the cause of failure can be identified through the use of metallurgical and mechanical testing, chemical and surface analysis data. Future

failures may be prevented by fixing or modifying the cause of a failure. This can be demonstrated in the example of a brittle fracture being the mode of failure. The corresponding cause of the brittle fracture may be temperature, presence of micro-cracks, or state of stress in the metal. In a failure analysis investigation, each question must be answered as completely as possible.

Determination of the mode of failure may be a relatively simple process for the failure analyst. However, identification of the exact cause of the failure is quite difficult, if not impossible, at times. The root cause of a failure in a complicated investigation may take months to determine, while a simple investigation may take only an hour depending upon the degree of complexity and the confidence level of the analyst. The investigation must be finely tuned; not too narrow and not too broad.

The following survey will present a logical method for failure analysis investigation; which will be applied to the mechanisms by which boiler tubes fail in service. Actual case histories are provided from the authors' many years of experience.

Methodology

Justification for conducting an investigation is an important issue for a failure analyst. Usually, justification for conducting the failure analysis investigation of a boiler tube is given in the identification of operational and material corrective actions for improved safety and operating efficiency. It may also be conducted for litigation related purposes in the event of suspected operational or material negligence.

If the investigation is fully justified, the method for evaluation proceeds with the second step in the process. This step involves gathering relevant information and facts concerning the failure. The questions listed serve as a guide to follow during the investigation. When the information has been obtained it must be carefully organized, labeled, and documented in a logical format for future reference.

The failure analyst should question why failure occurred, how to get the equipment back online as quickly as possible, how to prevent a recurrence, and if more information is needed, how the information can be readily obtained. With these steps taken a plan of attack can be formed. This is the single most important step in the method of evaluation. A logical plan for the investigation to follow must be developed and implemented. Each investigation will be different from the last and many variables will make it necessary to make decisions based on the investigation at hand. If an analyst is hasty in his decisions and does not have a solid plan, the analysis could be a waste of time. By simply cutting or analyzing a sample carelessly an analyst could destroy his only useful evidence.

Many possible tests and orders of application of tests for the identification of a failure mechanism are available. The selection made depends on the degree of precision required and the extensiveness of the range that has to be examined.

The stages of analysis performed when conducting a failure analysis investigation should begin with the collection of background data and sample removal. This step includes site inspection, information regarding the current history of the failure, all relevant record keeping, and statistics on past failures of the component.

Visual and Microscopic Examination

A preliminary visual examination of the failed part, as well as a non-destructive examination of the failure, with extensive photographic documentation, precedes any mechanical testing, including hardness and tensile testing, or any metallurgical examination. The preliminary examination does not change or damage the failed part in any way.

At this point in the investigation the specimens should be selected and identified for further laboratory testing and analysis. Management should be notified that any specimens taken from a failed component are often damaged, and of little use after testing.

There is a wide variety of testing methods currently available for failure analysis. Sophisticated and highly calibrated laboratory equipment can detect the slightest imperfections on a specimen, and accurately identify the inherent characteristics. The reference text of Brooks and Choudhury³ provides extensive discussion of analytical techniques to the failure analysis of materials in general.

A macroscopic examination of the surface of the selected specimen begins this stage of analysis, followed by a microscopic examination. This includes fracture surfaces, secondary cracks, discoloration, abnormalities, origin of fracture, and direction of the crack growth. In addition, corrosion product thickness, dimensional analysis, and level of deposit accumulation (via deposit-weight-density, DWD measurements) can also be evaluated.

Upon completion of the macroscopic and microscopic examination, a metallurgical analysis including etched and unetched, as well as transverse and longitudinal cross sections is conducted. This form of testing provides information on microstructural characteristics of the sample in failed and “good” areas, which allows for identification of the distinguishing characteristics.

Chemical Analysis Techniques

A chemical analysis of the metal and corrosion products utilizing x-ray fluorescence spectrometry (XRF), inductively coupled plasma spectroscopy (ICP), scanning electron microscopy (SEM) coupled with energy dispersive x-ray spectroscopy (EDS), x-ray diffraction (XRD), Fourier transform infrared spectroscopy (FTIR) for organic contamination studies, Auger electron spectroscopy (AES) and x-ray photoelectron spectroscopy (XPS) for surface characterization may follow the metallurgical analysis, depending on the investigation. All of these techniques are covered in more detail in the reference text by Sibilia⁴. Information from these different types of analyses may provide clues as to the cause of failure.

X-ray fluorescence spectrometry is a quantitative elemental analysis technique which uses x-rays to excite a sample. The excitation generates x-ray energies that identify the elemental composition of the sample. Using x-ray detection equipment to count the number of x-ray photons emitted by this technique, an x-ray fluorescence spectrometry system is able to characterize and quantify the elemental composition of the sample.

Inductively coupled plasma spectroscopy is an analytical technique used for the detection of dissolved metallic and non-metallic elements in aqueous solution. The primary physical operating principle of inductively coupled plasma spectroscopy is to get elements to emit characteristic wavelength specific light which can then be measured. It is an exceptionally useful analytical technique for the measurement of trace elements.

The scanning electron microscope is a microscope that uses electrons rather than light to form an image. There are many advantages to using the scanning electron microscope as an adjunct to the optical (light) microscope. The scanning electron microscope has a large depth of field, which allows a large amount of the sample to be in focus at one time. It also produces images of high resolution, which means that closely spaced features can be examined at a high magnification. Preparation of the samples is relatively easy since most scanning electron microscopes only require the sample to be electrically conductive.

Energy dispersive x-ray spectrometry systems are used in the characterization of materials through the use of ionizing radiation (electrons) to excite a sample. This excitation generates x-ray energies that identify the elemental composition of the sample. Using x-ray detection equipment to count the number of x-ray photons emitted by this technique, an energy dispersive x-ray spectrometry system is able to characterize and quantify in an approximate manner the elemental composition of the sample. Either used in conjunction with scanning electron microscopy imaging or on its own, the most common use for energy dispersive x-ray spectrometry in metallurgical analysis permits a general semi-quantitative determination of alloy, corrosion product, and contaminant chemistry.

X-ray diffraction is a powerful analytical technique relying on the constructive and destructive interference of x-rays diffracted from a sample that is illuminated by a filtered and focused beam of x-rays. If certain conditions are met then the intensity of the x-rays will be strong. These conditions provide information concerning the

spacing between planes of atoms in the crystal structure as well as a host of other details. X-ray diffraction is used to identify unknown materials in terms of their crystalline structure, and to look for deviations from the perfect structure which may indicate the presence of impurities, strain, the size of the crystal and other fine-scale structural defects.

Fourier transform infrared spectrometers record the interaction of infrared radiation (light) with experimental samples, measuring the frequencies at which the sample absorbs the radiation and the intensities of the absorptions. Determining these frequencies allows identification of the sample's chemical makeup, since chemical functional groups are known to absorb infrared radiation at specific frequencies.

Auger electron spectroscopy determines the elemental composition of conductive and semi-conductive surfaces, and can provide elemental depth profiles through sputtering. This information can then be utilized to solve problems associated with surface appearance, cleanliness and bonding. Additionally, corrosion products may be identified. In principle, an electron beam bombarding a solid surface excites electrons from core electronic energy levels of atoms. The kinetic energy spectrum is used to identify the atom of origin and its concentration.

X-ray photoelectron spectroscopy provides similar analyses offered by Auger electron spectroscopy and uses x-ray to excite core electrons, but it can be performed on a non-conducting surface, providing a definite advantage for organic materials and paints. X-ray photoelectron spectroscopy also may provide more detailed information on the binding state of an element, which provides the chemical bonds and the identity of compounds, which energy dispersive x-ray spectrometry and Auger electron spectroscopy cannot provide.

Fracture Mechanics

The analysis of fracture mechanics, including the measurement of fracture toughness and the evaluation of notch effects, provides information concerning the probability of a catastrophic failure under service conditions. Accelerated tests, as well as the recreation of the failure through simulated tests, confirm the proposed failure mechanism.

Analysis and Review of Evidence

Analysis of the evidence and a review of the existing data and documentation are the final stages of failure investigation. All information is gathered and analyzed to form a determination on the mode and probable cause of the failure. Identification of the mode and cause of failure provide the source for recommendations for corrective action. A final report including all relevant data, analyses, and recommendations are compiled and presented to the client. In litigation investigations, the client may not be interested in the recommendations section of the report.

Collection of Background Data

The failure analyst should determine when, where, and how the failure occurred. Interview all users and operators involved in the failure with point-related questions. Examples of point-related questions include "how was the part treated after failure?", "Was it protected?", "How was the fracture handled?", and "Did the failure involve overheating, which could have altered the microstructure of the weld or of the base metal?"

Sample Removal

The decision to remove a sample specimen is an important part of the failure analysis investigation. Samples selected should be characteristic of the material and contain a representation of the failure or corrosion attack. For comparative purposes, a sample should be taken from a sound and normal section. In conjunction, for a complete metallurgical examination of a failure, samples from the failure, adjacent to the failure, and away from the failure are necessary.

The sample must be removed without changing the surface conditions or characteristics of the sample, nor inflicting physical damage of any kind. The sample is the basis on which the investigation and analysis rely, and extreme care must be taken not to destroy any of the sample's properties.

Upon removal of the sample, the exact location on the piece of equipment from where it was taken must be clearly identified. The piece of equipment from which the sample was taken should also be identified and illustrated on an overall map of the area if possible.

To demonstrate the relationship of the sample and the piece of equipment a photograph should be taken. If more than one sample is to be taken, proper designation of the sample and its location relative to the piece of equipment should be noted and photographed. The dimensions of the sample and part specification should be noted on the photograph as well as the date the failure occurred.

Any corrosion product found on the coating or the substrate should be examined. If there is a corrosion product on the piece of equipment, but not on the sample, a representative sample of the corrosion product should be collected with the removed sample. However, if at all possible, the corrosion product/deposit should be kept intact on the surface, and not be separated from the sample. When the sample has been removed from the equipment it should be carefully wrapped and packaged in a tight box, identified and labeled.

There are many different ways that samples can be removed. Acetylene torch, air arc, saw, trepan, or drill can be used for the removal. All cuts made with an acetylene torch should be at least six inches from the area to be examined; cuts made by air arc should be at least four inches away.

If a cut were made closer to the area than stated, the heat generated could alter the microstructure, obscure the type of corrosive attack, or be cumulative to a failure, all of which would render the sample useless.

If the available distance for removal of the sample is less than four inches, the removal must be conducted with a saw or trepan. Drilling out the sample is also an option, but may dislodge deposits and corrosion product layers that need to be studied intact.

Proper removal and documentation of the sample, as well as information concerning the equipment, process, and service conditions are necessary. Important criteria that should be noted when a sample is removed are the date, equipment number, equipment process name, the manufacturer, heat treatment received, material of construction, environmental conditions (water treatment, temperature, pressure, and amount of time the equipment is used), and any abnormal service conditions existing at the time of the failure, or prior to the failure. This background information will provide the basis for a sound failure investigation.

ANALYSIS OF INDUSTRIAL FAILURES

Four case histories concerning boiler tube failures will be the focus of the following section. The case histories discussed include fatigue, erosion, short-term overheating, and hydrogen damage. The approach adopted for each case history will provide the principal characteristics of the failure, main identifying features, basic problem solving techniques, and applied aspects of the failures.

Industrial Case 1 - Fatigue

A failure analysis was conducted on one welded horizontal reheater lower bank tube assembly from a coal fired utility boiler identified as sample number 809. The sample was further identified as bundle number 188. The failed tube was identified as tube number 2 and the adjacent tube was identified as tube number 1. The tubes were specified to be 2.25 inch (57.2 mm) outside diameter (OD); 0.188 (4.78 mm) minimum wall thickness (MWT); American Society of Mechanical Engineers (ASME) SA 213 Grade A-1 material (UNS K02707). The tubes had been in service for only one year, with service conditions of 1010° F (543° C) and 800 psi (5.52 MPa).

The as-received reheater tube assembly is shown in Figure 1. The two tubes were joined together by tie bars that were welded to the tubes. Tube number 2 possessed a single circumferential crack that had propagated past the end of the tie bar weld at the weld toe location as shown in Figure 2. The end of the weld did not wrap around the end of the tie bar. The general arrangement of the welded assembly is shown in Figure 3. This cross section was cut approximately one inch behind the fracture surface. Failure of tube number 2 caused localized erosion of the tube number 1.

The failed tube was cut so that the mating fracture surfaces could be examined. The fracture surface was relatively flat and smooth textured. Series of parallel, closely spaced crack arrest marks were observed at several locations as shown in Figure 4. These features are characteristic of a fatigue mode of failure. The crack arrest marks were concentric about the fracture initiation location which was found to be at the weld toe location at the end of the weld. The mating fracture surfaces at the fracture initiation location are shown in Figure 5. The cluster of radially oriented ridges represents steps between separate, but closely spaced, fracture initiation sites.

One of the mating fracture surfaces was further examined at high magnifications using a scanning electron microscope. Some of the concentric crack arrest marks are shown in Figure 6. The underlying microstructural features of the steel tube were observed on the fracture surface where the rougher textured areas are the carbon rich bainite or pearlite phase, and the darker, smooth textured areas are the ferrite phase. Coarse crack arrest marks could be observed at some locations as shown in Figure 7. The average spacing between these observed crack arrest marks was measured to be approximately 0.07 mm. No finer spaced fatigue striations could be observed between the coarser spaced crack arrest marks. Therefore, it was not possible to calculate the number of elapsed cycles since the fracture initiated.

A transverse cross section through the fracture initiation location, parallel to the length of the weld, was prepared for subsequent metallographic examination. Etching with a 2% nital solution revealed the existing microstructures. The fracture initiation site at the weld toe location is shown in Figure 8. The microstructure of the heat affected zone (HAZ) is shown in Figure 9 and consisted of dark etching bainite plus white etching ferrite. The microstructure of the failed tube away from the weld is shown in Figure 10 and consisted of dark etching pearlite in a matrix of white etching ferrite. No microstructural evidence of overheating of the boiler tube steel was observed at locations away from the weld. The microstructure of the weld metal deposit consisted of darker etching carbides in a white etching ferrite matrix. The microstructure of the tie bar consisted of numerous small dark etching carbides in a white etching ferrite matrix.

In the lightly etched condition a Knoop microhardness inspection, using a 500 g load, was performed in the HAZ, weld metal, and the base metal of the failed tube. Knoop microhardness measurements ranged from 165–212 (80–92 HRB) in the HAZ, 224–255 (95 HRB – 21 HRC) in the weld metal, and 159–168 (78–81 HRB) in the base metal.

A quantitative chemical analysis was performed on the failed tube, tie bar, and the weld metal joining the tie bar to the failed tube. The failed tube conformed to the chemical requirements of ASME SA 213 Grade A-1 plain carbon steel (UNS K02707). The tie bar nearly conforms to the chemical requirements of ASME SA 213 Grade T22 ferritic alloy steel (UNS K21590), except that the measured phosphorus content is greater than the specified maximum value. The weld metal deposit could not be matched with any standard American Welding Society (AWS) electrode composition, most likely due to dilution with the base metal.

The failure of the reheater tube occurred as a result of high cycle fatigue which initiated on the outside diameter surface of the tube, at the weld toe location, at the end of the weld joining the tie bar to the failed tube. The weld did not wrap around the end of the tie bar, and so there was excessive stress concentrated at the weld toe location. The weld joint failure is a complex issue which is being further investigated. It is believed at this point that flow induced vibrations may be causing the failure. The investigation is still underway, and may take several more months to pin down the root cause and corrective actions.

Industrial Case 2 – Erosion

One rear waterwall tube from a coal fired utility boiler which had failed in service was analyzed to determine the cause of failure. The tube was identified as: sample number 782. The sample was further identified as: tube number 255, number 5 burner crotch tube at elevation 784. The tube was specified to be 1.75 inch (44.5 mm) OD, 0.200 inch (5.1 mm) MWT, ASME SA 210 material (UNS K02707).

The window failure in the waterwall tube is shown in Figure 11. The window was measured to be approximately 6.81 inches (173 mm) long. The failure occurred approximately 3.5 inches (89 mm) from a circumferential weld. Along one of the 6.75 inch (171 mm) long edges of the window the fracture surface was observed to be approximately 0.21 inch (5.3 mm) thick. Along the other 6.75 inch (171 mm) long edge of the window the fracture surface was observed to be only approximately 0.03 inch (0.8 mm) thick. On the opposite side of the tube from the window failure the tube wall thickness was measured to be approximately 0.22 inch (5.6 mm). Outward plastic deformation of the fracture surfaces was observed along both long edges of the window fracture as shown in Figure 11. Shallow corrosion pitting was observed on the inside diameter (ID) tube surfaces as shown in Figure 12. Thick oxide scale deposits were observed on the outside diameter OD surface on the side of the tube where the failure had occurred.

A cross section through the fracture was made and the wall thickness profiles for the tube at the fracture locations are shown in Figure 13. The rupture of the tube had produced an outward plastic deformation of the tube wall. A second cross section through the tube at a location away from the failure was also made. The tube wall thickness profile at this location is shown in Figure 14. Approximately 30% loss of wall thickness was observed on the fireside surface in the tube as shown in cross-sectional view in Figure 14, at the 2 o'clock position.

A quantitative chemical analysis of the failed tube material was performed. The failed tube did conform to the specified chemical requirements of ASME SA 210 Grades A-1 and C material (UNS K02707 and UNS K03501).

Transverse cross sections were made through the fracture surfaces on both sides of the window failure, and also through non-failed areas of the tube for comparison purposes. In the as polished condition, corrosion pitting was observed on the inside diameter surface of the tube around the entire circumference. The pitting appeared to be deepest on the failed side of the tube. The maximum pit depth at this plane of section was measured to be 0.38 mm inches. An example of a deep corrosion pit is shown in Figure 15. The thinner fracture surface is shown in Figure 16. All of the corrosion pit surfaces were observed to possess a thin layer of high temperature iron oxide indicating that the corrosion pits were not likely to be active. The wall thickness at the fracture location was measured to be only 0.025 inch (0.62 mm).

Localized necking, or plastic deformation, was observed on the OD surface immediately adjacent to the fracture as shown in Figure 16. In addition, many small black voids were observed within the metal, across the entire tube wall thickness immediately adjacent to the fracture surface. These features are characteristic of a tensile overload mode of failure. A cross section through the tube away from the fracture, but in line with the area of reduced wall thickness, was also prepared for examination. The minimum wall thickness at this location was measured to be 0.108 inch (2.74 mm). The thicker fracture surface, on the other side of the window failure, is shown in Figure 17. This fracture surface exhibited a slanted profile characteristic of a ductile shear mode of failure. The wall thickness at this fracture location was measured to be 0.167 inch (4.24 mm). Secondary cracks were observed to have initiated on the ID surface close to the primary fracture location as shown in Figure 18. The larger of the secondary cracks also exhibited a slanted profile. The thickness of the scale layer on the OD tube surface is shown in Figure 19. The maximum OD scale thickness was measured to be 0.081 inch (2.06 mm). Spherical particles of fly ash were observed in the outermost layers of the scale deposits. No evidence of internal sulfidation or oxidation was observed within the tube metal at the metal/scale interface.

Etching with a 2% nital solution revealed the existing microstructures. On the opposite side of the tube from the window failure the tube microstructure was found to consist of dark etching pearlite in a matrix of white etching ferrite as shown in Figure 20. The pearlite usually occurred in bands. The microstructure of the tube at the thinner wall fracture location is shown in Figure 21. A slight elongation of the microstructure was observed

immediately adjacent to the fracture surface. The microstructure at this location consisted of dark etching pearlite in a matrix of white etching ferrite. No evidence of overheating was observed. The microstructure of the tube at the thicker wall fracture location is shown in Figure 22. The microstructure at this location consisted of dark etching pearlite in a matrix of white etching ferrite. Again no evidence of overheating was observed. The microstructure of the tube at the location of the secondary cracks is shown in Figure 23. Localized plastic deformation was observed in the vicinity of the secondary cracks. The outside diameter surface of the tube, in a region of reduced wall thickness, is shown in Figure 24. The OD tube surface exhibited a smooth profile and intersected the pearlite bands at an angle as shown in the photographs. This is evidence of erosion of the OD surface of the tube.

The failure of the waterwall tube, sample number 782, produced a window shaped opening in the tube. Cross sectional views and metallographic examination revealed a considerable reduction in tube wall thickness especially on one side of the window shaped opening. Metallographic evidence indicated that the reduction in wall thickness of the tube occurred primarily as a result of localized erosion and oxidation of the OD tube surface. The erosive particles are believed to be fly ash as much fly ash was observed within the OD scale deposits adjacent to the location of failure. The final failure then occurred as a result of a tensile overload. In this case, the fly ash problem is not a design or operational problem. This was just routine fly ash erosion after many years in service.

Industrial Case 3 – Short –Term Overheating

One reheater tube sample was submitted for failure analysis from the horizontal reheater assembly front wall (row 94, tube 2) of a power station number 1 coal fired boiler. The tube was further identified as sample number 816. The tube was specified to be 2.375 inch (60.33 mm) OD; 0.400 inch (10.16 mm) MWT; ASME SA 213 grade T2 material (UNS K11547). The tube had been in service for over thirty years, with service conditions of 1010° F (543° C) and 800 psi (5.52 MPa).

The as-received horizontal reheater assembly front wall boiler tube is shown in Figures 25 and 26. The tube possessed one large window failure as shown in Figure 25. The two longitudinal fracture surfaces did not mate together indicating that a section of the failed tube is missing. One of the fracture surfaces exhibited localized tube wall thinning while the second fracture retained its original tube wall thickness. Two longitudinal wear marks were observed on the OD surface adjacent to the thicker fracture surface. These marks suggest that the tube ruptured violently and struck an external object causing a thicker, secondary fracture of the tube. The thinner fracture surface is shown in Figures 27. Slanted shear lips, characteristic of a tensile mode of failure, were observed. The thicker walled fracture surface is shown in Figure 28.

It was observed that the wall thickness of the failed tube was less on the side of the tube that was in line with the thin walled fracture surface. See Figure 29. The outside diameter surface was observed to be relatively smooth in texture all around the tube circumference. Oxidation of the outside diameter surface had occurred, but no erosion was found, that would contribute to the decrease in observed wall thickness. The OD of the tube at the location shown in Figure 29 was measured to be between 2.500 and 2.702 inches (63.50 mm and 68.63 mm) versus a specified OD of 2.375 inches (60.33 mm). The increase in diameter indicates overheating and swelling of the tube. The minimum wall thickness shown in Figure 29 was measured to be 0.268 inch (6.81 mm) versus a minimum specified wall thickness of 0.400 inch (10.16 mm). The maximum wall thickness shown in Figure 29 was measured to be 0.412 inch (10.46 mm).

A transverse cross section through the thinner fracture surface was prepared for subsequent metallographic examination. The macroscopic appearance of the fracture is shown in Figure 30. In the as-polished condition shallow corrosion pitting was observed along the outside diameter surface. Shallow secondary cracks were also observed as shown in Figure 31. The fracture surface profile is shown again in Figure 32. Numerous elongated internal fissures were observed within the steel immediately adjacent to the fracture as shown in Figure 32. Many of these fissures were coincident with nonmetallic inclusions. The presence of internal fissures at nonmetallic inclusions is characteristic of a tensile overload mode of failure.

Etching with a 2% nital solution revealed the existing microstructure which was found to consist of dark etching bainite and martensite plus white etching ferrite as shown in Figures 33 and 34. The microstructure in the immediate vicinity of the fracture was found to be highly elongated due to the occurrence of localized plastic deformation. The microstructure of the tube away from the fracture surface is shown in Figure 35 and consisted of dark etching bainite in a matrix of white etching ferrite. The microstructure was not elongated at this location. The fracture surface profile, microstructure elongation, and presence of internal fissures at nonmetallic inclusions are characteristic of a tensile mode of failure.

A transverse cross-section through the thicker fracture surface was also prepared for metallographic examination. The macroscopic appearance of the fracture profile is shown in Figure 36. The fracture at this location had initiated at the OD surface as indicated by the presence of a slanted shear lip adjacent to the ID surface. No evidence of plastic deformation was observed at this location. The microstructure at this location consisted of dark etching islands of bainite and martensite in a white etching ferrite matrix as shown in Figure 37.

A transverse cross-section through the thinnest observed wall thickness away from the fracture, as shown in Figure 29, was also prepared for metallographic examination. The microstructure at this location consisted of dark etching islands of bainite and martensite in a matrix of white etching ferrite as shown in Figure 38. The microstructure at this location displayed a slight elongation. The microstructure of the tube at a location 180° away, on the opposite, thickest walled area is shown in Figure 39 and consisted of dark etching bainite and martensite plus pearlite in a matrix of white etching ferrite.

The presence of martensite and bainite plus ferrite in the tube microstructures indicates overheating of the tube metal within the temperature range of 1320° F (715° C) to 1650° F (900° C).

A quantitative chemical analysis was performed on the failed tube. The failed tube did conform to the chemical requirements of ASME SA 213 Grade T2 ferritic alloy steel (UNS K11547).

The horizontal reheater assembly front wall boiler tube failed as a result of a ductile stress overload failure caused by rapid short-term overheating. Rapid overheating in turn is caused by high tube metal temperatures and low steam flow through the tube. In the present instance the failure was promoted by the occurrence of a low tube wall thickness on the side of the tube that experienced failure (Figure 29). Creep expansion thinned the wall, and the creep rupture resulted in the failure by ductile stress overload at elevated temperatures.

Industrial Case 4 – Hydrogen Damage

One section of a boiler tube that had experienced corrosion of the inside diameter surface that led to perforation of the tube wall thickness was analyzed. The sample was identified as number 2 boiler; rear wall tube sample number 712. The rear wall tube was reportedly inclined and the corrosion occurred at the 12 o'clock position. The tube material was specified to be 3.00 inch (76.2 mm) OD, 0.250 inch (6.35 mm) MWT, ASME SA 210 material (UNS K02707). The tube had reportedly been in service for approximately 260,000 hours, or over 29 years, with service conditions of 750° F (400° C) and 190 psi (13.10 MPa). The tubes were last chemically cleaned in 1995 using the chelant EDTA. We were requested to determine the mechanism of internal corrosion.

The outside diameter surface of the as received tube section is shown in Figures 40 and 41. All of the visible surfaces had been surface ground. The inside diameter surface of the as received tube section is shown in Figure 42. A large area of deep corrosion pitting accompanied by thick oxide scale layers at some locations was observed. Cracking was observed at the bottoms of the deepest corroded areas as shown in Figure 43. White colored deposits were observed around the periphery of and underneath the thicker black oxide scale layers.

The corrosion products within the corroded area of the inside diameter surface were further analyzed for their elemental compositions using a scanning electron microscope (SEM) equipped with an energy dispersive x-ray spectrometer (EDS). A spectrum of the brown deposit covering much of the inside diameter surface is shown in Figure 44. An EDS spectrum of the thick black scale was obtained and was confirmed to be iron oxide. An EDS spectrum of the white colored deposit was obtained and was found to contain iron (Fe), phosphorus (P), oxygen

(O), carbon (C), aluminum (Al), silicon (Si), copper (Cu), and zinc (Zn) plus lesser amounts of sulfur (S), calcium (Ca), and manganese (Mn).

A transverse cross section through the secondary crack in the tube was prepared for subsequent metallographic examination. In the as polished condition, the scale deposit on the inside diameter (ID) surface of the tube, in a non corroded area is shown in Figure 45. The scale layer contained a considerable number of metallic copper particles. At locations where the tube wall thickness exhibited reduced values due to corrosion, cracking and void formation was observed adjacent to the ID surface that extended almost all of the way across the tube wall thickness. See Figure 46. Etching with a 2% nital solution revealed the existing microstructure which consisted of dark etching islands of pearlite in a matrix of white etching ferrite as shown in Figure 47. The microstructure within the damaged area is shown in Figure 48. The tube wall thickness at the secondary crack was measured to be 0.116 inch (2.95 mm). The tube wall thickness away from the corrosion pitted area was measured to be 0.214 inch (5.44 mm).

A quantitative chemical analysis of the tube material was performed. The tube did meet the specified chemical requirements of either Grade A-1 (UNS K02707) or Grade C (UNS K03501) of ASME SA 210.

The tube failed as a result of hydrogen damage which had initiated in a portion of the tube that had experienced a considerable decrease in wall thickness due to corrosion of the inside diameter surface. The corrosion, in turn, may have been caused by a localized acidic corrosion cell.

CONCLUSION

This paper emphasized the basic problems and applied aspects of the corrosion and metallurgical failures of boiler tubes. Four separate types of failures were presented detailing the factors and mechanisms affecting the failures. Fatigue failures result in fracture initiation and propagation. Erosion failures lead to wall thinning and subsequent tensile overload. High tube metal temperatures lead to rapid short-term overheating, which in turn results in ductile stress overload. Hydrogen damage can be due to excessive tube metal temperatures or wall thinning from corrosion.

REFERENCES

1. D.N. French, Metallurgical Failures in Fossil Fired Boilers, Second Edition, New York, NY: John Wiley & Sons, Inc., 1993.
2. R.D. Port and H.M. Herro, The NALCO Guide to Boiler Failure Analysis, New York, NY: McGraw-Hill, Inc., 1991.
3. C.R. Brooks and A. Choudhury, Failure Analysis of Engineering Materials, New York, NY: McGraw-Hill Companies, Inc., 2002.
4. J.P. Sibilias, A Guide to Materials Characterization and Chemical Analysis, Second Edition, New York, NY: Wiley-VCH, Inc., 1996.



FIGURE 1 - Photograph showing the as received reheat tube assembly.



FIGURE 2 - Photograph showing the circumferential crack in tube no. 2.



FIGURE 3 - Photograph showing the geometry of the welded assembly.



FIGURE 4 - Photograph showing parallel fatigue crack arrest marks on the fracture surface.

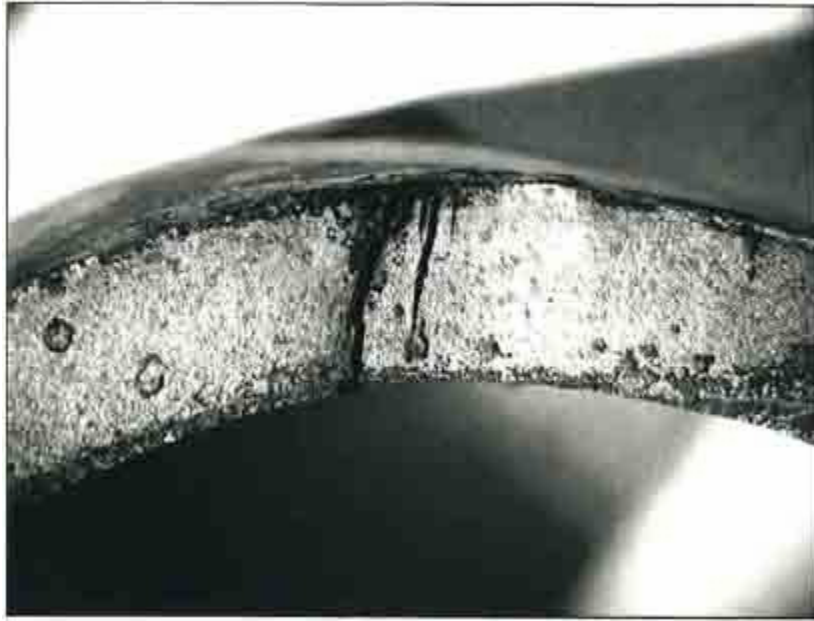


FIGURE 5 - Photograph showing one of the mating fracture initiation sites.



FIGURE 6 - Scanning electron micrograph at 14x showing fatigue crack arrest marks adjacent to the fracture initiation location.



FIGURE 7 - Scanning electron micrograph at 245x showing a series of fatigue crack arrest marks.

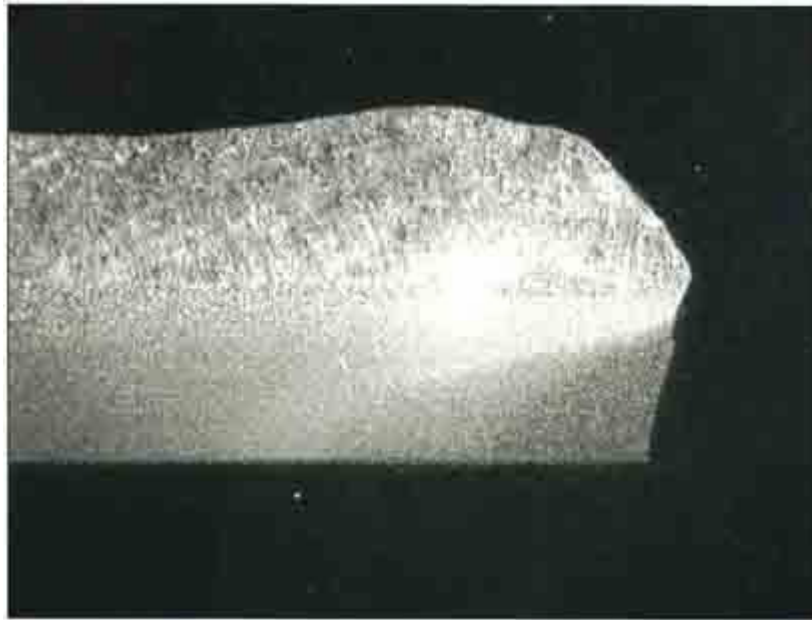


FIGURE 8 - Photograph at 8x showing the fracture initiation site at the weld toe location. 2% nital.



FIGURE 9 - Photograph at 400x showing the microstructure of the heat affected zone (HAZ); 2% nital.



FIGURE 10 - Photograph at 400x showing the base metal microstructure; 2% nital.

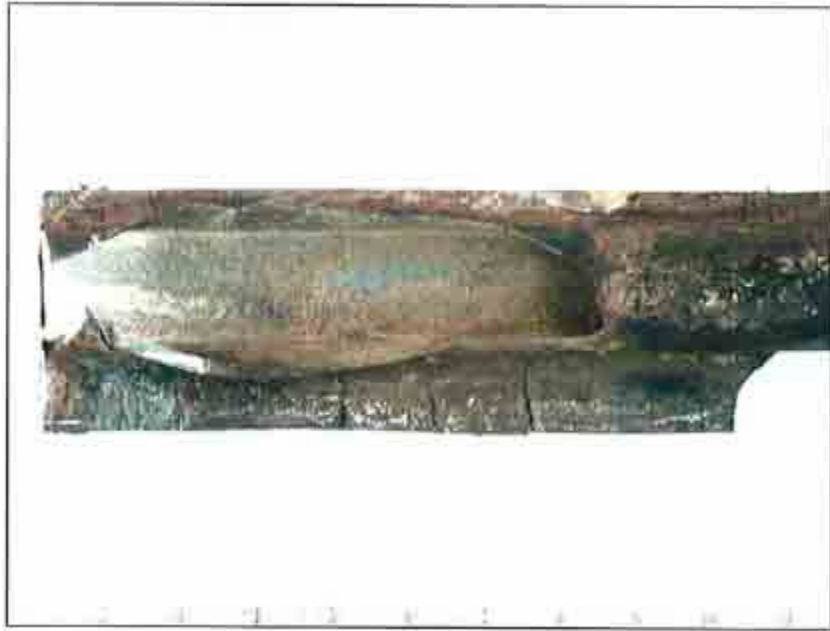


FIGURE 11 - Photograph at 1.4x showing the window failure in the waterwall tube.



FIGURE 12 - Photograph at 8x showing shallow corrosion pitting of the ID tube surface.

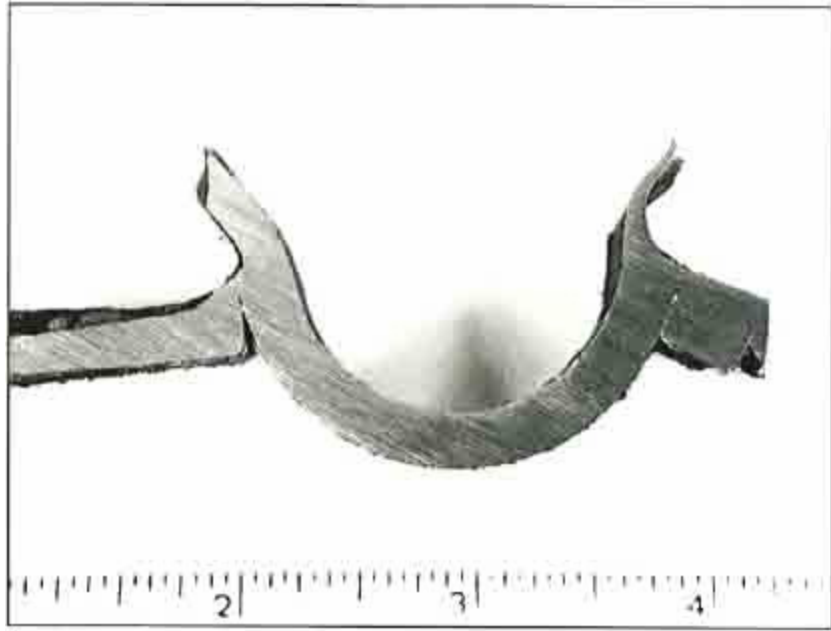


FIGURE 13 - Photograph at 2x showing the tube wall thickness profile at the location of failure.



FIGURE 14 - Photograph at 2x showing the tube wall thickness profile away from the location of failure.

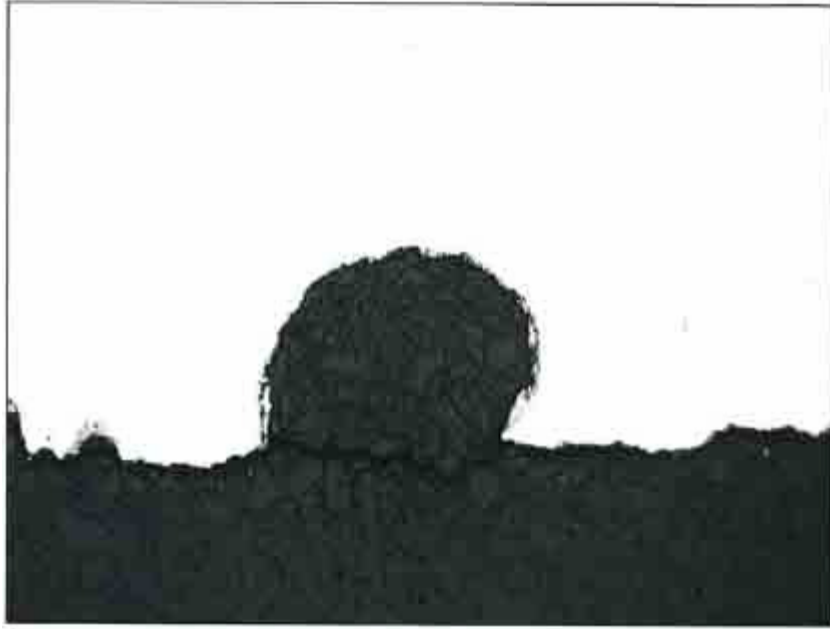


FIGURE 15 - Photograph at 100x showing corrosion pitting at the ID surface of the tube; as polished.

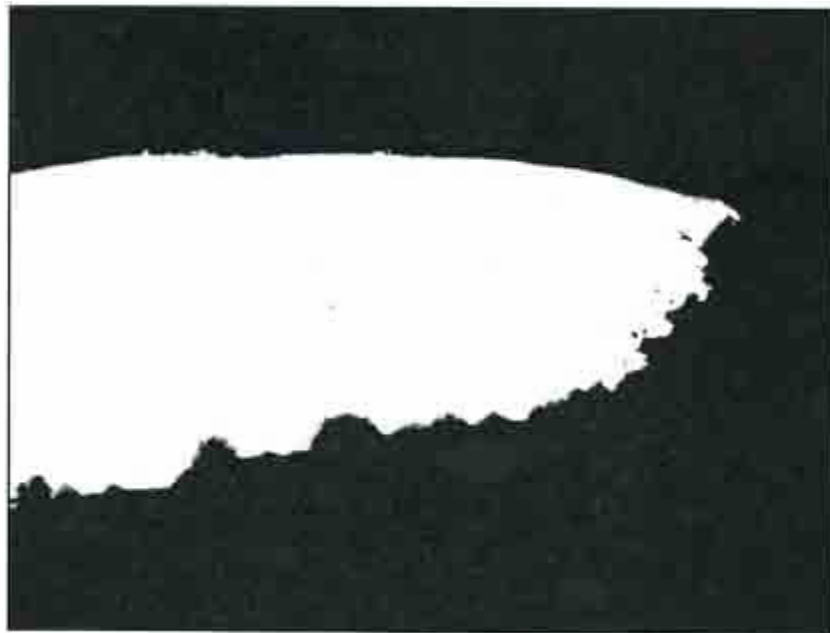


FIGURE 16 - Photograph at 50x showing the thinner fracture surface profile; as polished.

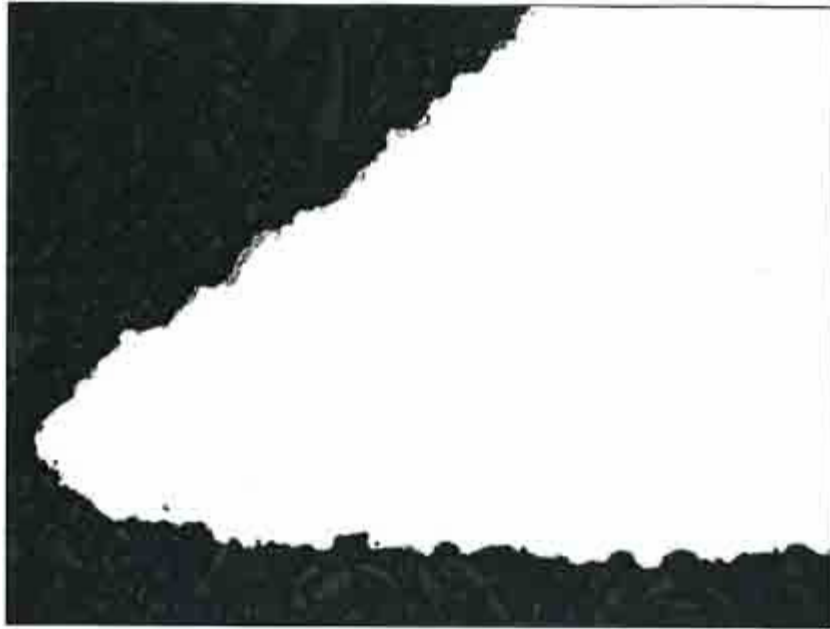


FIGURE 17 - Photograph at 50x showing the thicker fracture surface profile at the ID surface; as polished.

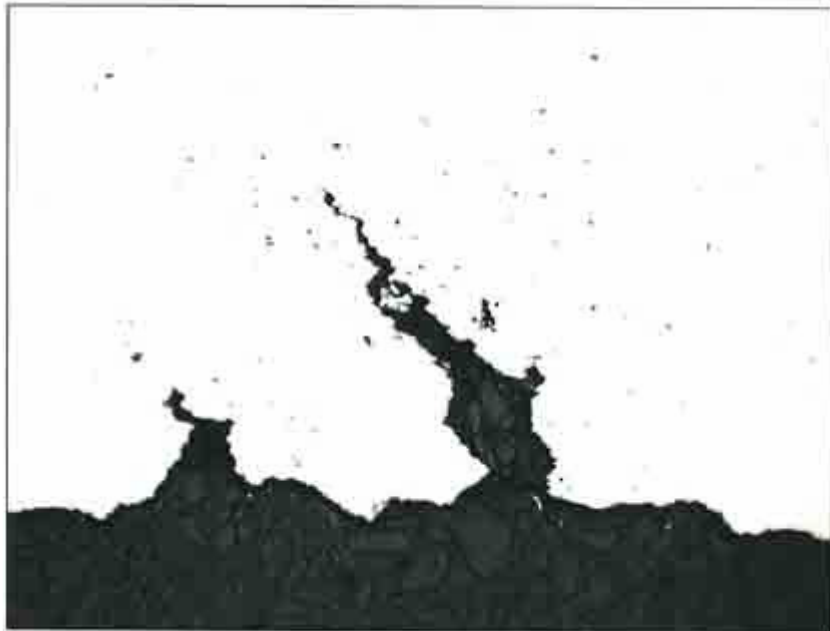


FIGURE 18 - Photograph at 100x showing secondary cracks initiating at the ID tube surface; as polished.

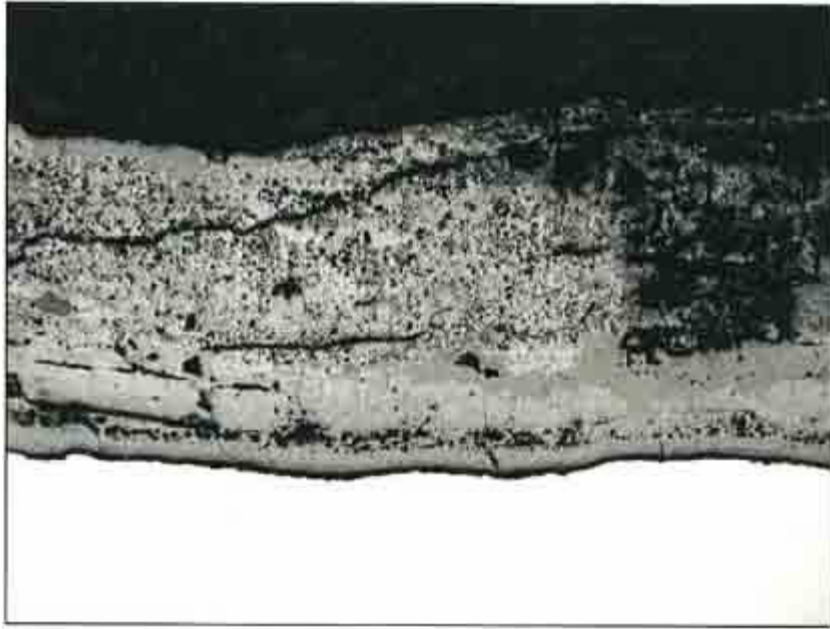


FIGURE 19 - Photograph at 50x showing the scale deposits on the OD tube surface; as polished.



FIGURE 20 - Photograph at 400x showing the microstructure of the tube away from the failure; 2% nital.

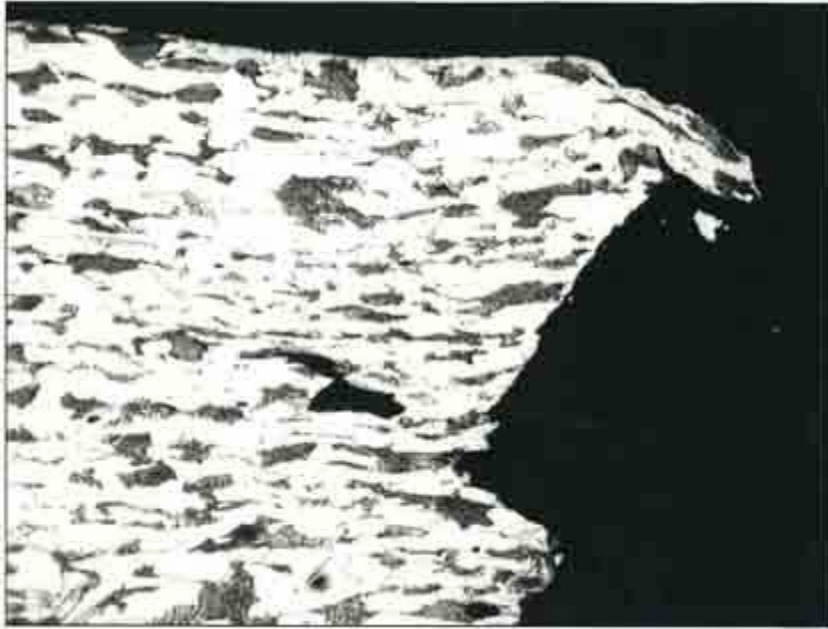


FIGURE 21 - Photograph at 400x showing the tube microstructure at the thinner fracture surface; 2% nital.

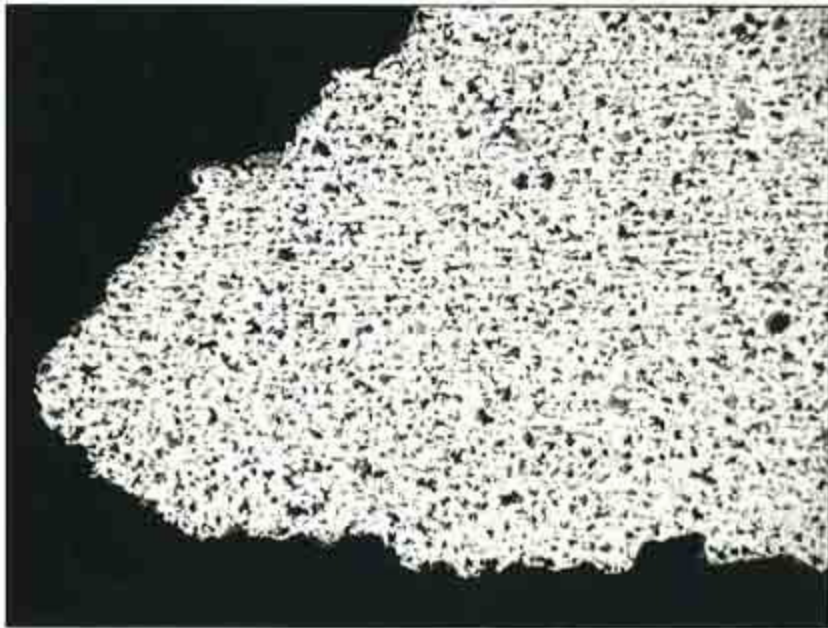


FIGURE 22 - Photograph at 100x showing the tube microstructure of the thicker fracture at the OD surface; 2% nital.

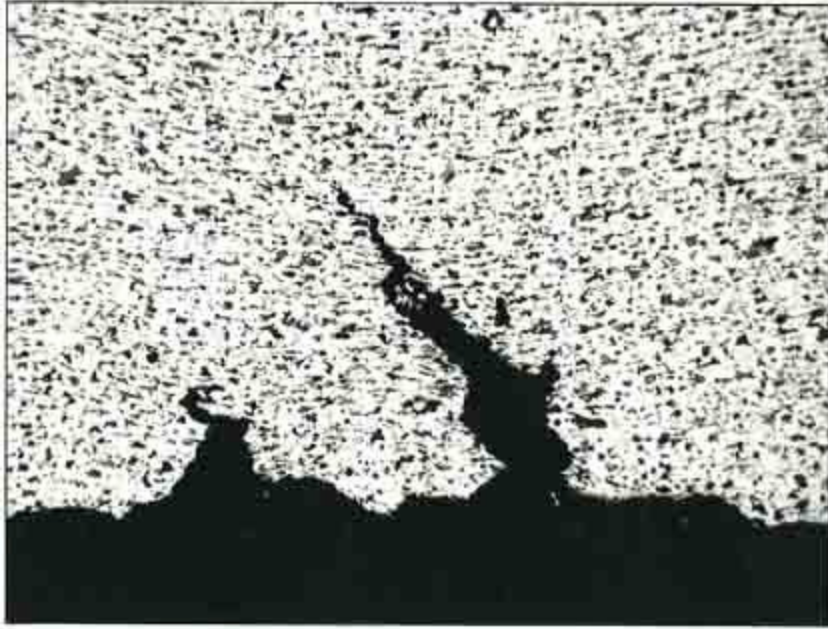


FIGURE 23 - Photograph at 100x showing the tube microstructure at the location of the secondary cracks; 2% nital.



FIGURE 24 - Photograph at 400x showing the smooth eroded OD surface profile of the tube; 2% nital.



FIGURE 25 - Photograph showing the as received horizontal reheat assembly front wall boiler tube.



FIGURE 26 - Photograph showing the as received horizontal reheat assembly front wall boiler tube.

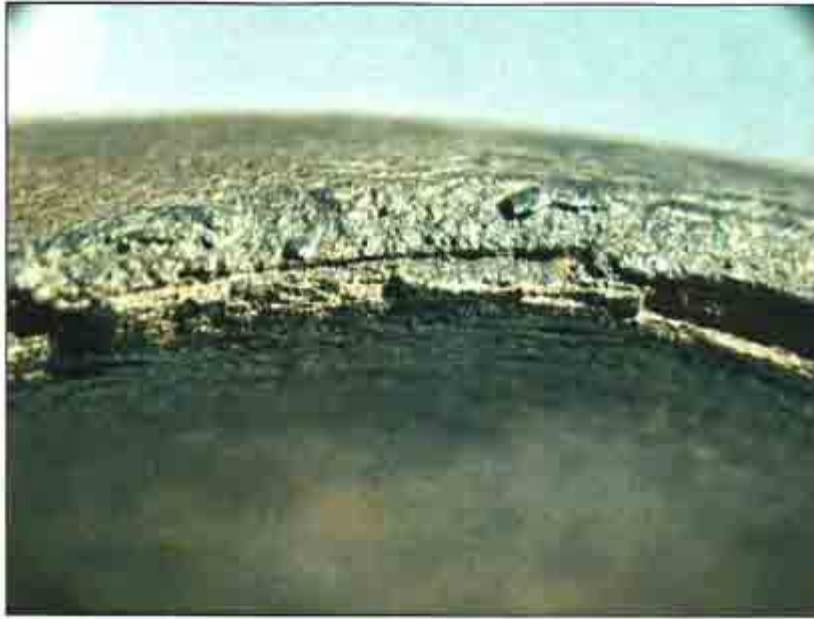


FIGURE 27 - Photograph at 8x showing the thinner walled fracture surface.



FIGURE 28 - Photograph at 8x showing the thicker walled fracture surface.

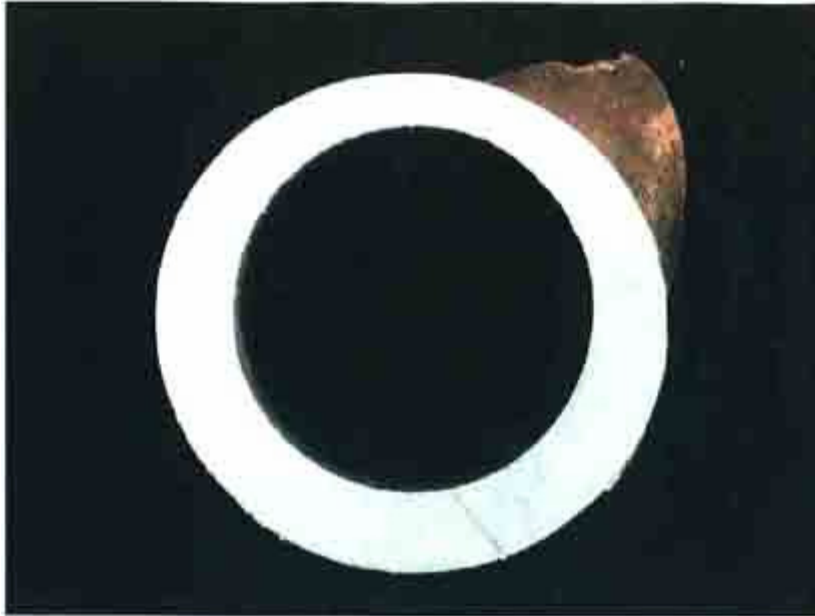


FIGURE 29 - Photograph showing the non uniform tube wall thickness.



FIGURE 30 - Photograph at 8x showing the thin walled fracture surface profile; 2% nital.

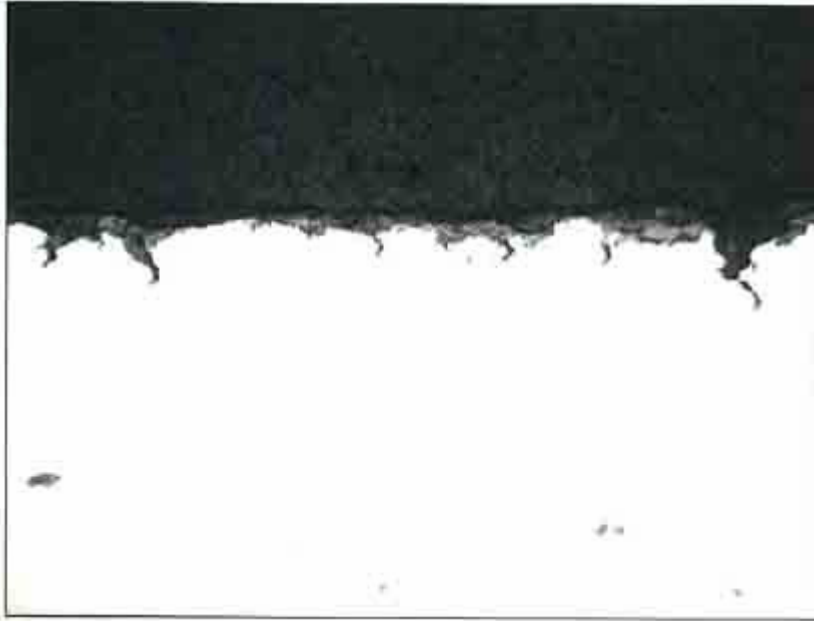


FIGURE 31 - Photograph at 400x showing secondary cracks near the fracture at the OD tube surface; as polished.

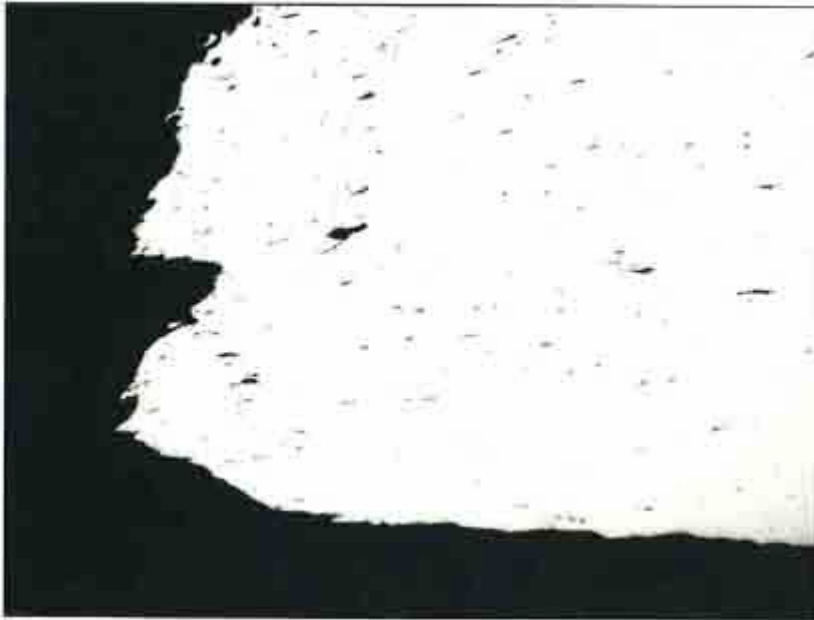


FIGURE 32 - Photograph at 50x showing the thin wall fracture profile at the ID surface; as polished.

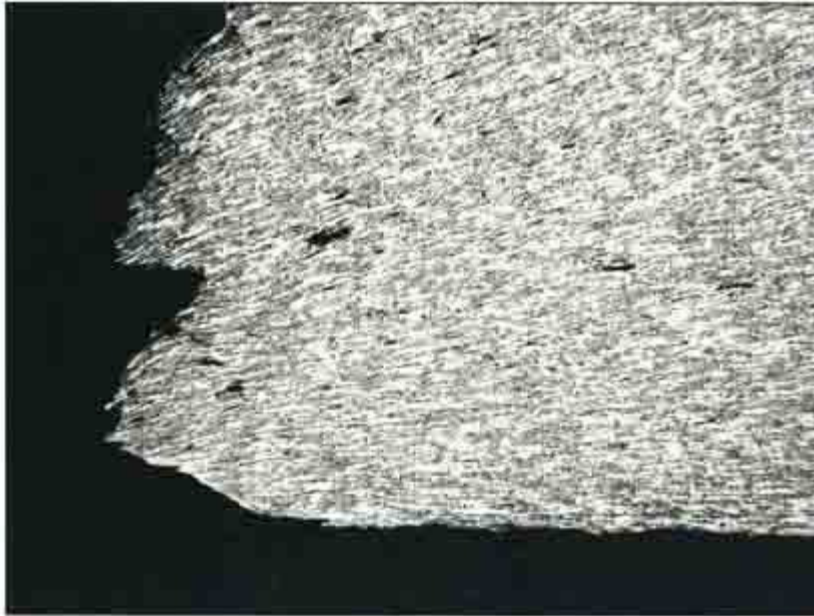


FIGURE 33 - Photograph at 50x showing the thin wall fracture profile at the ID surface; 2% nital.

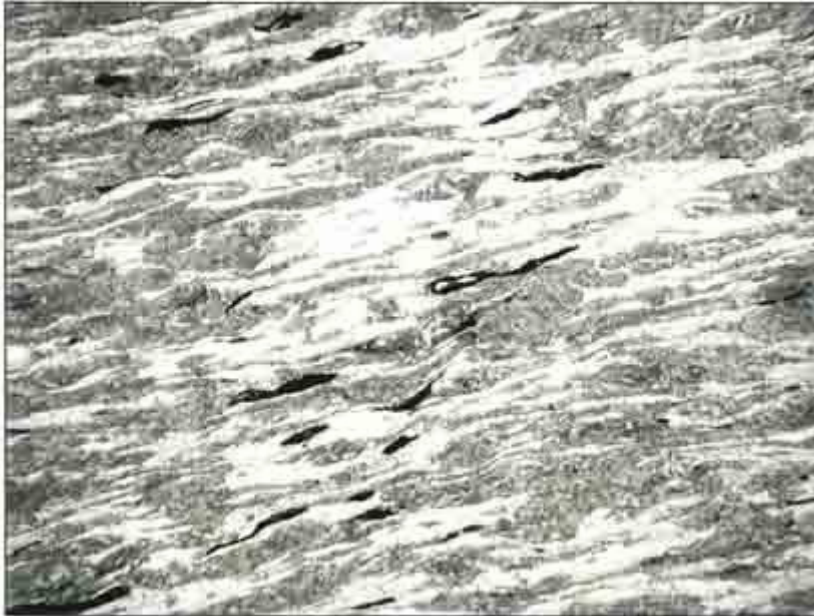


FIGURE 34 - Photograph at 400x showing the tube microstructure adjacent to the thin wall fracture; 2% nital.



FIGURE 35 - Photograph at 1000x showing the tube microstructure away from the thin wall fracture; 2% nital.

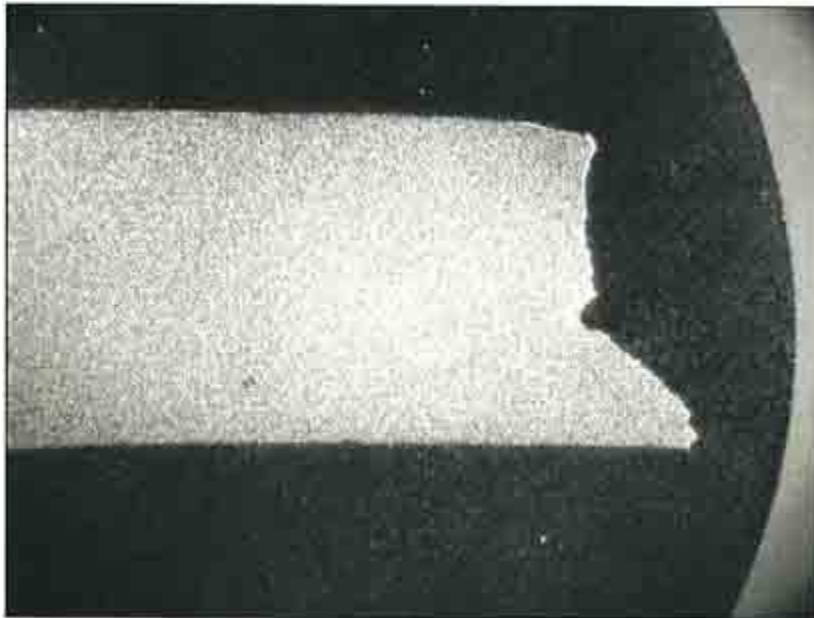


FIGURE 36 - Photograph at 8x showing the thick wall fracture surface profile; 2% nital.



FIGURE 37 - Photograph at 200x showing the tube microstructure near the thick wall fracture; 2% nital.

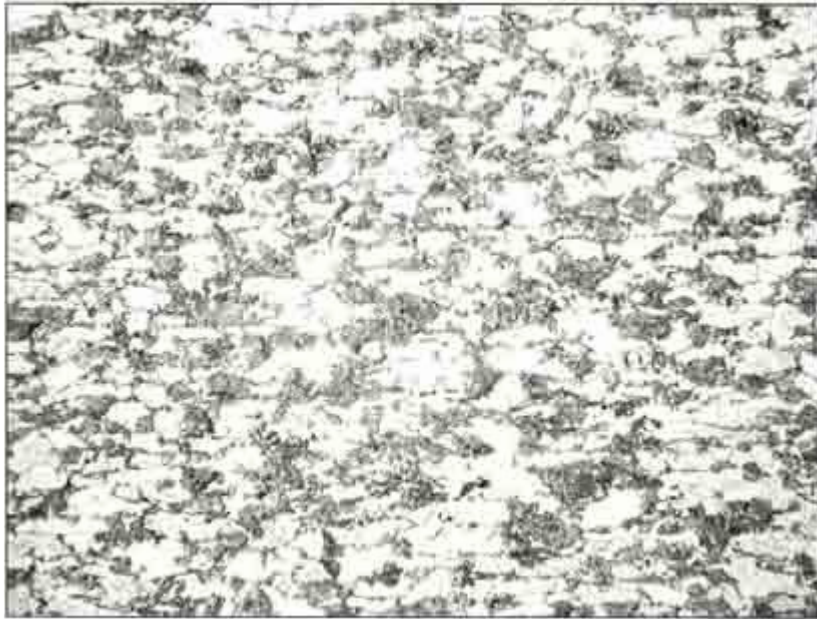


FIGURE 38 - Photograph at 200x showing the tube microstructure away from the fracture in the thinnest wall area; 2% nital.

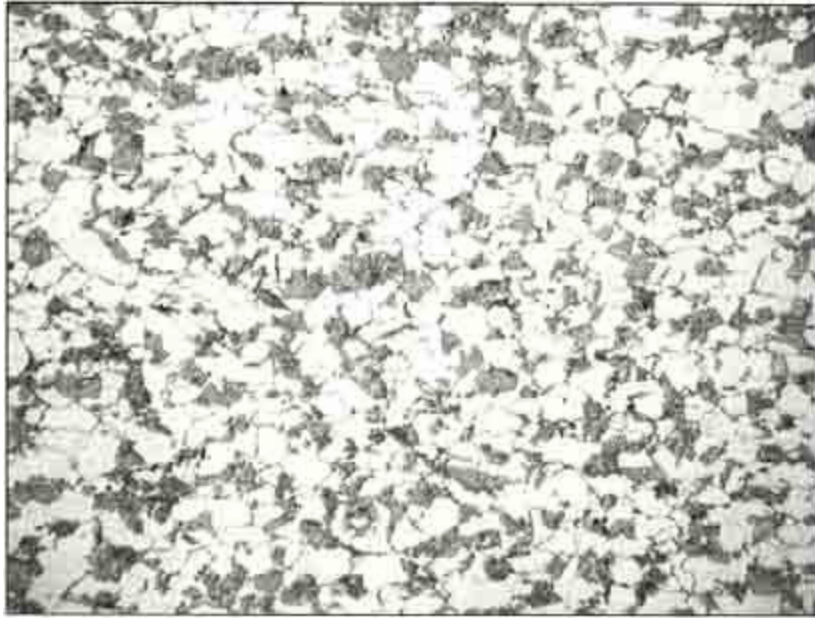


FIGURE 39 - Photograph at 200x showing the tube microstructure away from the fracture in the thickest wall area; 2% nital.



FIGURE 40 - Photograph showing the OD surface of the as received tube section.



FIGURE 41 - Photograph showing the perforation in the tube wall thickness at the OD surface.



FIGURE 42 - Photograph showing the ID surface of the as received tube section.



FIGURE 43 - Photograph showing the perforation in the tube wall thickness at the ID surface.

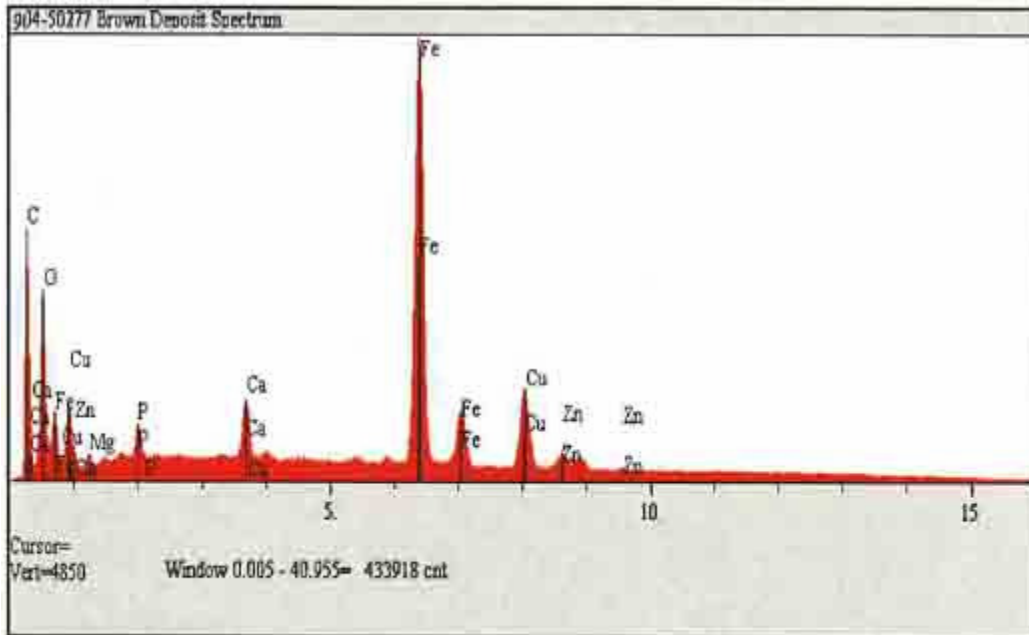


FIGURE 44 - EDS spectrum of the brown colored ID deposit.

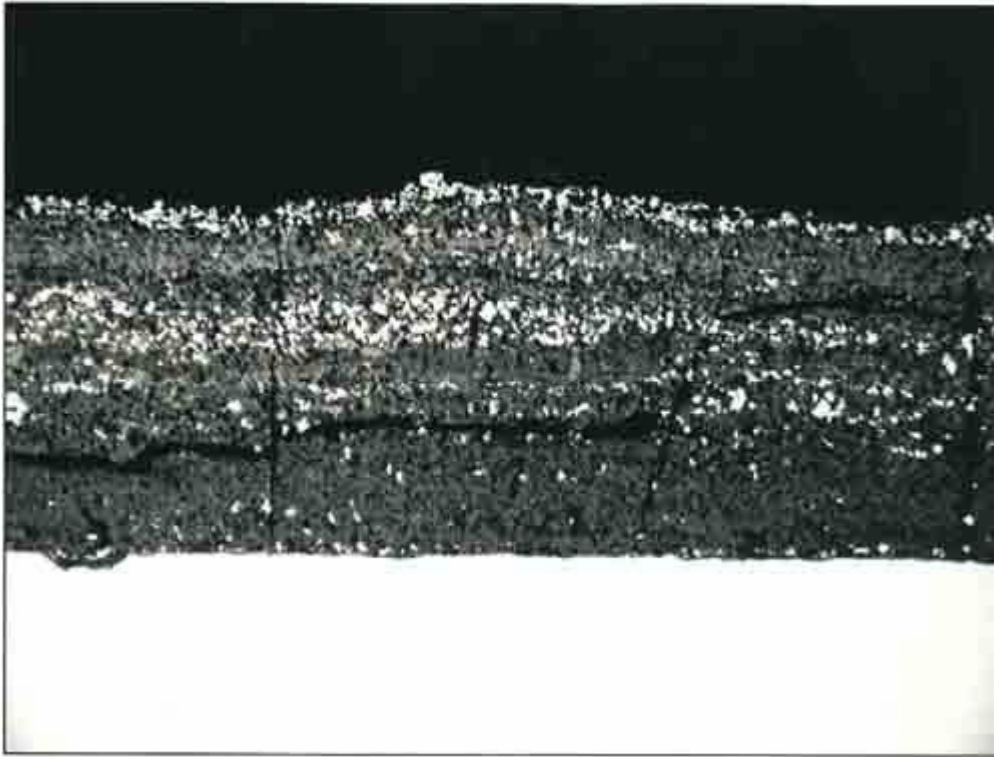


FIGURE 45 - Photograph at 200x showing the ID oxide scale layer; as polished.



FIGURE 46 - Photograph at 50x showing cracking and hydrogen damage void formation; as polished.

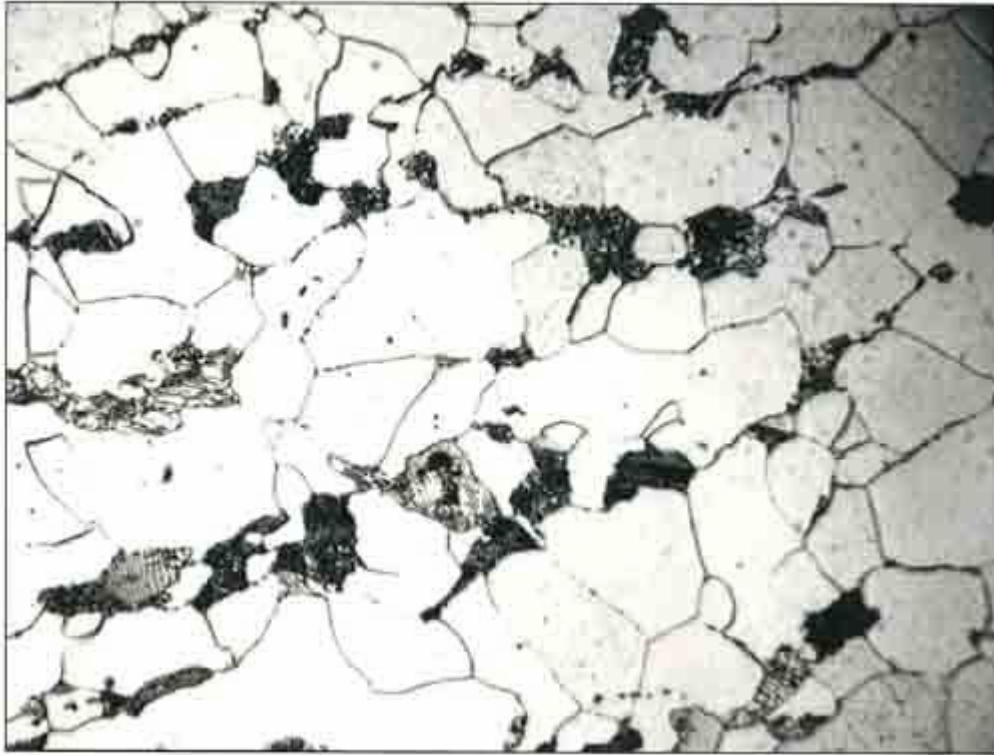


FIGURE 47 - Photograph at 1000x showing the microstructure of the tube; 2% nital.



FIGURE 48 - Photograph at 1000x showing the microstructure of the tube in the hydrogen damaged area; 2% nital.